JOURNAL OF APPLIED ELECTROCHEMISTRY **27** (1997) 325–334

Corrosion and corrosion inhibition of alumina particulate/aluminium alloys metal matrix composites in neutral chloride solutions

C. MONTICELLI, F. ZUCCHI, G. BRUNORO, G. TRABANELLI

Corrosion Study Center "A. Daccò", Department of Chemistry, University of Ferrara, I-44100 Ferrara, Italy

Received 2 January 1996; revised 17 July 1996

A study of the corrosion behaviour and corrosion inhibition of AA 6061 and AA 2014 metal matrix composites (MMCs) reinforced with alumina particles, during exposures to 0.1 M NaCl solution is reported. Many tungsten and molybdenum-containing inorganic salts were tested as corrosion inhibitors, but only ammonium tetrathiotungstate afforded good inhibiting properties, particularly towards the AA 2014-based MMC. The corrosion behaviour of the composites in uninhibited or inhibited solutions was compared by different techniques to that exhibited by the corresponding matrices. The techniques adopted included weight loss measurements, electron probe microanalysis (EPMA), scanning electron microscopy (SEM), linear polarization resistance measurements, polarization curve recordings and current noise analysis. The analysis of the current fluctuations showed that different patterns of the time records were obtained during pit initiation, stable pitting and general corrosion. The power spectrum density plots exhibited $f^{-\alpha}$ trends, with α values around 20 dB decade^{-1} when corrosion was mainly localized in pits, while values tending to zero were measured when general corrosion became dominant.

1. Introduction

Metal matrix composites (MMCs) were developed to produce materials with higher Young's modulus/density and yield strength/density ratios, together with a tailorable coefficient of thermal expansion and high thermal stability and conductivity. These improved properties are often achieved at the expense of a lower corrosion resistance, as the reinforcing particles or fibres introduce inhomogeneities on the surfaces exposed to aggressive environments. This is particularly evident when the matrix is an active metal, such as aluminium and its alloys, and the reinforcement has electrical conductivity or semiconductivity, as in the case of graphite or silicon carbide. In these cases, the presence of galvanic cells will stimulate the corrosion process on the matrix. Alumina is an insulator and alumina particles or fibres can be used to reinforce aluminium alloys without inducing galvanic corrosion. However, previous studies carried out on pure aluminium reinforced with alumina short fibres (Saffil) also suggested that the introduction of this reinforcement could adversely affect the corrosion behaviour, by introducing flaws in the surface passive film [1]. Therefore, it is of interest to study the corrosion behaviour of two alumina-reinforced aluminium alloys MMCs.

Many substances have been tested as corrosion inhibitors of these materials and their corresponding matrices. Among these were salts of tungsten and molybenum-containing anions, selected following the paper of Lomakina *et al.* [2], who studied the corrosion inhibition of aluminium alloys by addition of iso- and heteropoly anions of these two elements in high temperature water, containing a low chloride and sulfate concentration.

2. Experimental details

The 20% Al_2O_{3p}/AA6061-T6 and 10% Al_2O_{3p}/AA 2014-T6 studied were particulate reinforced MMCs. The matrices were aluminium alloys (Table 1). The average particulate size was 18 μm. Each electrode was fabricated by inserting an insulated copper wire into a small hole drilled on one sample side. The electrical joint was protected by epoxy resin, so that the sample surface exposed to the solutions was that opposite to the contact. The electrode surfaces were ground mechanically with emery paper and polished with diamond paste (3 μm). They were then rinsed with distilled water and degreased with acetone. Finally, they were partially masked with resin to produce electrode areas of 0.3–1 cm^2. The electrodes for noise measurements were prepared with areas of 5.7 cm^2. Small coupons of the different materials (about 10 cm^2 of exposed surface area; finishing: 600 emery paper) were also prepared for weight loss measurements.

The test solution was a 0.1 M NaCl solution, kept at the temperature of 25°C. The different materials were compared by recording their anodic and cathodic polarization curves in the test solution, after 1 day of immersion, at a potential scanning rate of 0.1 mV s^{-1}.

0021-891X

Table 1. Nominal compositions of the studied aluminium alloys

	Cu	*Fe*	*Si*	*Mg*	*Mn*	*Zn*	*Ti*	*Cr*
AA 6061	0.25	(0.7)	0.6	1	(0.15)	(0.25)	(0.15)	(0.25)
AA 2014	4.4	(0.5)	0.8	0.4	0.8	(0.1)	(0.1)	(0.1)

Values in parentheses refer to the higest tolerable content.

Many substances were tested as corrosion inhibitors: sodium molybdate dihydrate, sodium tungstate dihydrate, ammonium tetrathiotungstate, ammonium tetrathiomolybdate, ammonium (*para*)-tungstate, ammonium (*meta*)-tungstate hydrate, sodium polytungstate, phosphotungstic acid hydrate, phosphomolybdic acid and tungstosilicic acid hydrate. All were supplied by the Aldrich Chem. Co. They were used at a concentration of 1 g dm^{-3}. The pH values of the solutions containing the last three substances were adjusted by sodium hydroxide additions, in order to shift them to the range 5.5–6.0. The screening of the different substances as corrosion inhibitors was carried out by recording the anodic and cathodic polarization curves, mainly on AA 6061-T6 eletrodes, after 1 day of immersion (potential scanning rate 0.1 mV s^{-1}).

The most promising substances were tested on all the investigated materials and the weight losses obtained after 1 month of exposure to the aggressive solution were also evaluated. At the end of the immersion, scanning electron microscopy (SEM) and electron probe microanalysis (EPMA), mainly on cleaned samples, were performed. The cleaning process was according to [3].

The corrosion behaviour of the MMCs and their matrices was monitored during 5 day immersions in uninhibited and inhibited solutions, by analysing the electrochemical current noise obtained between two 'identical' electrodes. The current fluctuations were detected by means of a home-made zero resistance ammeter. Data acquisition (4096 data, 0.03 s interval) was performed by a high resolution multimeter (HP 3457A) connected to a Compaq Prolinea 4/66 through an IEEE 488 National Instruments interface. After linear trend removal, the data were transformed by a fast Fourier transform algorithm into power spectrum density (PSD) plots, ranging from 8×10^{-3} to 16 Hz. Each plot was the average of four plots, obtained from four consecutive time records. Noise power values in the frequency range 0.1–10 Hz were also calculated.

The results of the electrochemical noise analysis were compared to measurements of linear polarization resistance, R_p, taken during the 5 days of immersion, in the potential range $E_{corr} \pm 5$ mV, at a scanning rate of 0.1 mV s^{-1}.

All the potentials quoted in the text are referred to the saturated calomel electrode (SCE).

3. Results

3.1. *Polarization curves*

Figures 1 and 2 compare the polarization curves obtained on AA 6061-T6 MMC and AA 2014-T6 MMC, respectively, after 1 day of immersion in 0.1 M NaCl solution (solid curves). The matrices exhibited polarization curves close to those obtained on the corresponding composites.

The cathodic curves are strongly dependent on the copper content of the alloy, so that a strong stimulation of the oxygen reduction process is noticed on AA 2014-T6 MMC and its matrix, relative to AA 6061-based materials. The shift of the cathodic polarization curves of AA 2014-based materials towards higher current densities makes the corrosion potentials about 100 mV nobler than those of AA 6061-based materials. In all cases, the pitting potentials are more or less coincident with the corrosion potentials.

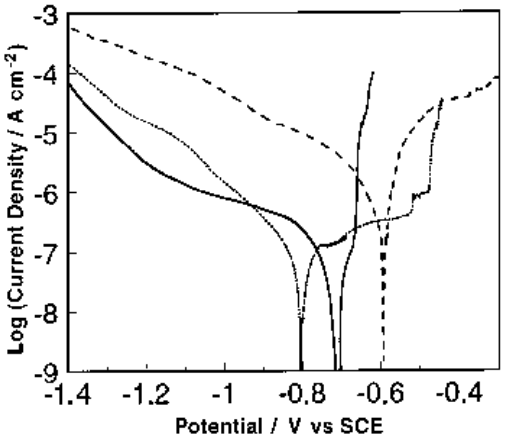

Fig. 1. Polarization curves recorded on AA 6061-T6 MMC after 1 day of immersion in 0.1 M NaCl, in the absence (solid line) or in the presence of the following additives: tetrathiotungstate (dotted line); tetrathiomolybdate (dashed lines).

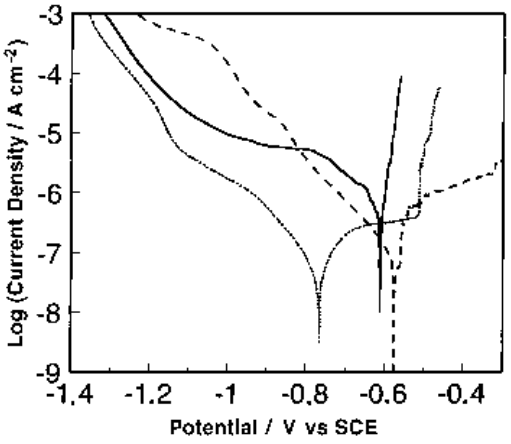

Fig. 2. Polarization curves recorded on AA 2014-T6 MMC after 1 day of immersion in 0.1 M NaCl, in the absence (solid line)or in the presence of the following additives: tetrathiotungstate (dotted line); tetrathiomolybdate (dashed lines).

Table 2. Weight losses (in mdd) obtained after one month of exposure of the different materials in 0.1 M NaCl, in the absence and in the presence of tetrathiotungstate or tetrathiomolybdate

	AA 6061-T6	AA 6061-T6 MMC	AA 2014-T6	AA 2014-T6 MMC
0.1 M NaCl	2.16	1.06	6.64	7.08
0.1 M NaCl + thiotungstate	0	0	0	0
0.1 M NaCl + thiomolybdate	1.90	6.34	1.58	1.99

All the inorganic substances tested, except ammonium tetrathiotungstate, not only failed in inhibiting the anodic and cathodic processes on AA 6061-T6, but also stimulated the reduction process.

Figures 1 and 2 also compare the E/log i characteristics of the composites, obtained in the blank solution, to those recorded in the presence of tetrathiotungstate (dotted curves). A clear inhibition of the anodic process on both composites and of the cathodic process on the AA 2014-T6 MMC is achieved. However, the measurement on AA 6061-T6 MMC electrodes, of lower corrosion potential in inhibited than in uninhibited solution, suggests that an inhibitive effect on the reduction process is also obtained on this material. The pitting potentials in the presence of tetrathiotungstate are shifted to −0.520 V, in both cases, with a width of the passive potential range of about 300 and 250 mV, for AA 6061-T6 MMC and AA 2014-T6 MMC, respectively. The curves recorded on the matrices were similar.

Owing to its similarity to the tetrathiotungstate anion, tetrathiomolybdate was also tested as corrosion inhibitor for both alloys and the corresponding MMCs. Figures 1 and 2 show that a fair inhibiting effect is only achieved on AA 2014-T6 MMC (dashed curves). On AA 6061-T6 MMC, it produces a kind of passive region on the anodic polarization curve, characterized by high passive current densities. In both cases, the anion shifted the corrosion potentials of the composites in the noble direction. The matrices exhibited an analogous behaviour.

3.2. *Weight losses and EPMA*

Table 2 shows the weight losses obtained on the different materials in the absence and in the presence of the two most promising inhibitors. In the blank solution, the much higher corrosion rates of the materials with a high copper content are noticed.

Moreover, the results of the gravimetric test suggest a higher corrosion resistance of AA 6061-T6 MMC with respect to its matrix and the slightly higher corrosion resistance of AA 2014-T6 with respect to the corresponding composite.

The SEM observations and EPMA carried out on cleaned samples of the various materials after 5 days and 1 month of exposure to the blank solution were aimed at investigating this opposite behaviour. AA 6061-T6 showed a few pits and a diffused micropitting attack, mainly localized around small precipitates, containing particularly iron, but also copper and chromium in traces (Fig. 3). The spot analysis of the integer regions only detected the elements typical of the alloy, that is aluminium, silicon and a little magnesium. In contrast, AA 6061-T6 MMC showed isolated small pits localized besides alumina particles (Fig. 4) and EPMA only revealed the presence of the main alloying elements.

Also in the case of AA 2014-based materials, the presence of intermetallic precipitates, containing copper, iron and manganese, besides aluminium, was only visible on the matrix and induced a uniform extensive micropitting, after 5 days of immersion (Fig. 5). However, these elements were found to be

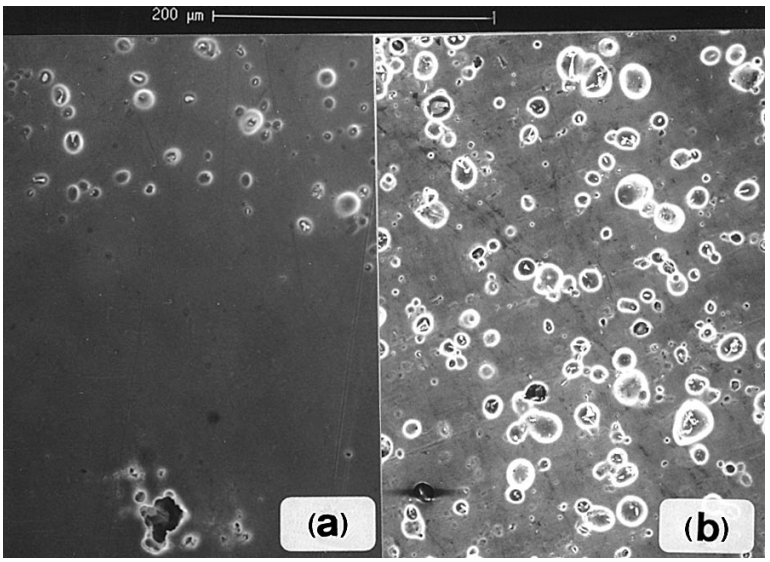

Fig. 3. SEM micrographs obtained on AA 6061-T6, after 5 days (a) and 30 days (b) in 0.1 M NaCl.

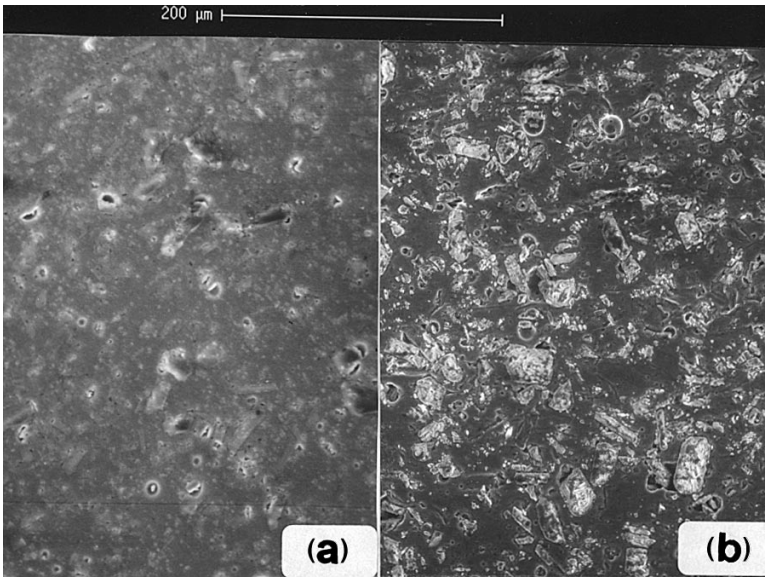

Fig. 4. SEM micrographs obtained on AA 6061-T6 MMC, after 5 days (a) and 30 days (b) in 0.1 M NaCl.

present more or less uniformly at every point on the surfaces of both the matrix and the composite specimens. The localization of the pitting attack was different: on the matrix, beside micropitting, a few intergranular cracks began to form after 5 days of immersion in the aggressive solution and became clearly evident after 1 month of exposure (Fig. 5), while, on the composite, the localized attack appeared to start mainly around reinforcing particles, as for AA 6061-T6 MMC (Fig. 6).

Table 2 shows that tetrathiotungstate was an excellent corrosion inhibitor. It blocked any localized attack. In contrast, tetrathiomolybdate slowed down the corrosion process of AA 2014-T6 MMC and its matrix only slightly, without avoiding pitting corrosion, as evidenced by a visual observation of the specimens.

The presence of tungsten and, particularly, molybdenum on the surface of uncleaned specimens after 1 month exposure to the inhibited solution was confirmed by EPMA. The presence of a few particles containing sulfur and not molybdenum, after exposure to the tetrathiomolybdate solution, was detected only on AA 6061-T6 MMC.

3.3. *Polarization resistance measurements*

The trends of the reciprocal values of the polarization resistance values ($1/R_p$) during the 5 days of immersion, in the absence and in the presence of tetrathiotungstate, are shown in Fig 7 and 8, which refer to the AA 6061-based material and to the AA 2014-based materials, respectively. The inhibitive action of tetrathiotungstate is evident in both figures, but particulary in Fig. 8.

During the immersion of AA 6061-based materials in the blank solution, the corrosion potentials shifted from −0.8 V, measured after 2 h, up to −0.700/−0.660 V, after 1 day, and remained more or less constant to the end of the immersion. In inhibited solution, these materials exhibited quite lower corrosion potentials (−0.87 V, 2 h of immerison; −0.75/

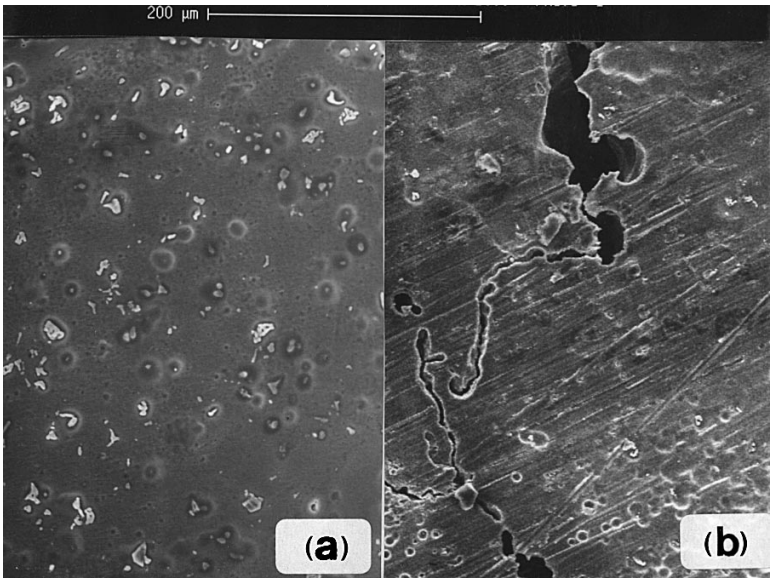

Fig. 5. SEM micrographs obtained on AA 2014-T6, after 5 days (a) and 30 days (b) in 0.1 M NaCl.

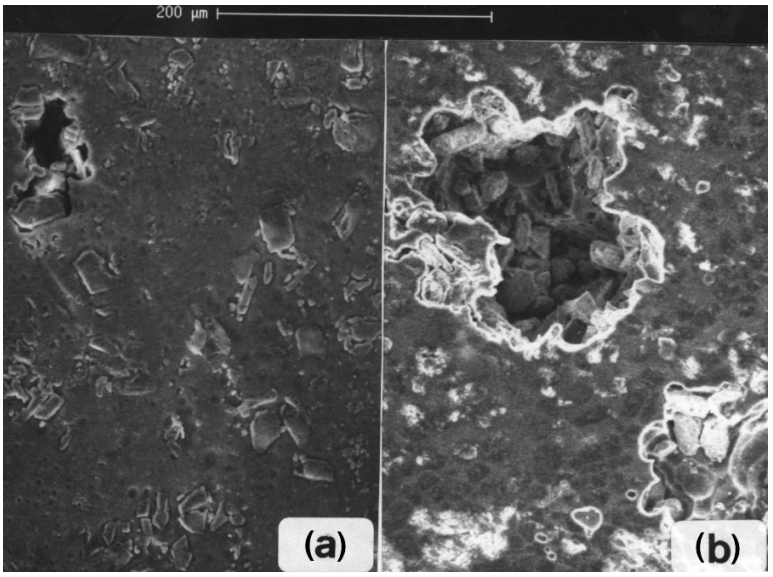

Fig. 6. SEM micrographs obtained on AA 2014-T6 MMC, after 5 days (a) and 30 days (b) in 0.1 M NaCl.

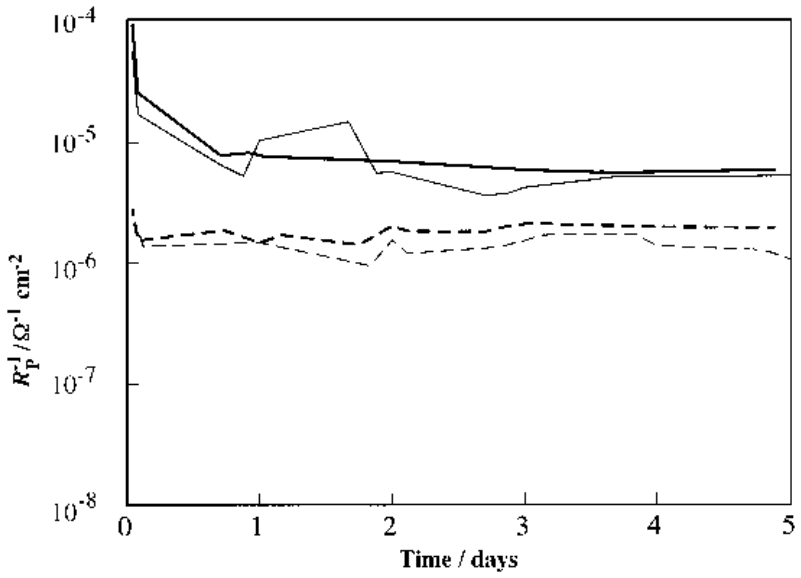

Fig. 7. Reciprocal values of the polarization resistance values, measured at different immersion times in 0.1 M NaCl, in the absence and in the presence of tetrathiotungstate. Key: (——) AA 6061 blank; (- - - -) AA 6061 inhib.sol.; (——) AA 6061 MMC blank; (- - - -) AA 6061 MMC inhib.sol.

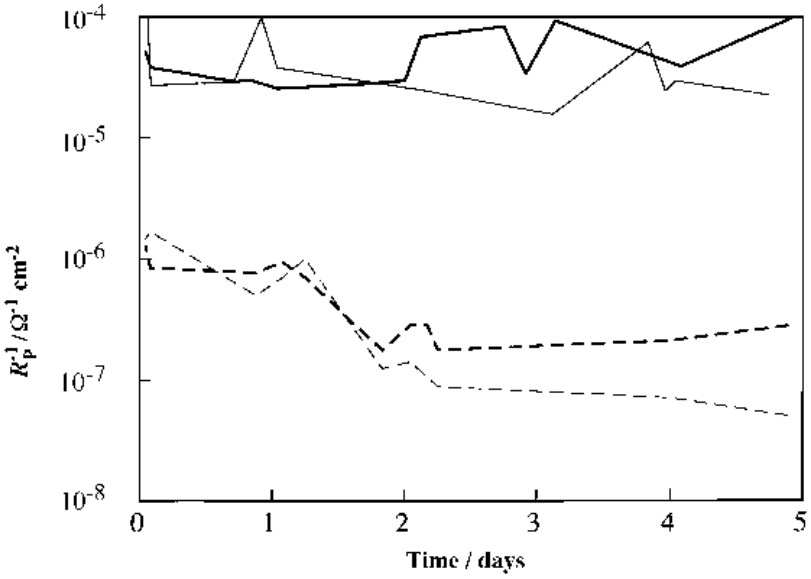

Fig. 8. Reciprocal values of the polarization resistance values, measured at different immersion times in 0.1 M NaCl, in the absence and in the presence of tetrathiotungstate. Key: (——) AA 2014 blank; (- - - -) AA 2014 inhib.sol.; (——) AA 2014 MMC blank; (- - - -) AA 2014 MMC inhib.sol.

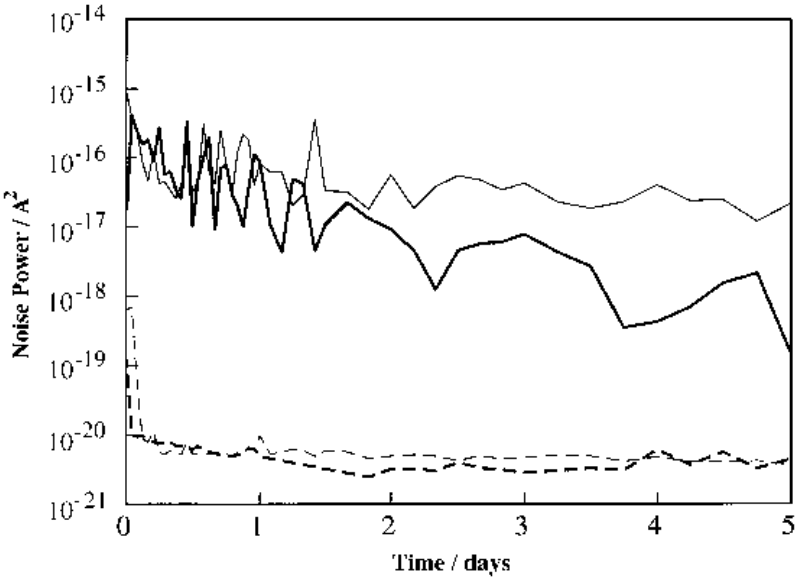

Fig. 9. Noise power values, measured at different immersion times in 0.1 M NaCl, in the absence and in the presence of tetrathiotungstate. Key: (——) AA 6061 blank; (- - - -) AA 6061 inhib.sol.; (——) AA 6061 MMC blank; (- - - -) AA 6061 MMC inhib.sol.

−0.8 V, 5 days of immersion), indicating a limitation in the growth of the passive film.

In the blank solution, the corrosion potentials of AA 2014-based materials oscillated between −0.700 and −0.630 V, during all the immersion period, with an initial value of −0.575 V for AA 2014-T6, recorded after 2 h of immersion. In the presence of tetrathiotungstate, they initially decreased down to −0.75 V, then, after about 1.5 days of immersion, they settled around −0.7/−0.68 V, to the end of the immersion. Therefore, the inhibitor did not shift the corrosion potential, but stabilized it.

3.4. *Current noise analysis*

The noise power values obtained during the 5 day immersion are shown in Figs 9 and 10. In the blank solution AA 6061-T6 exhibits very discontinuous noise power values, during the first day of immersion (Fig. 9). Then, these values stabilized around 3×10^{-17} A^2. Initially, the composite produces comparable noise power values, but after 1 day they tend to decrease. Figure 10 shows for the AA 2014-based materials that the composite exhibits higher and more oscillating noise power values, than the matrix.

The analysis of the time records at different immersion times was useful to monitor the evolution of the corrosion process with time. During the first hours, continuously oscillating current/time records were obtained and no clear cutoff frequency can be obtained from the PSD plots: the composites exhibit $f^{-\alpha}$ trends of the PSD plots, with α values around 18–19 dB decade^{-1}, over the whole frequency range, while the matrices show analogous trends at high frequencies and decreasing α values in the lowest frequency decade.

The time records and corresponding spectra obtained at 1 day of immersion are reported in Fig. 11. The AA 6061-based materials afford current–time patterns similar to each other: they are characterized

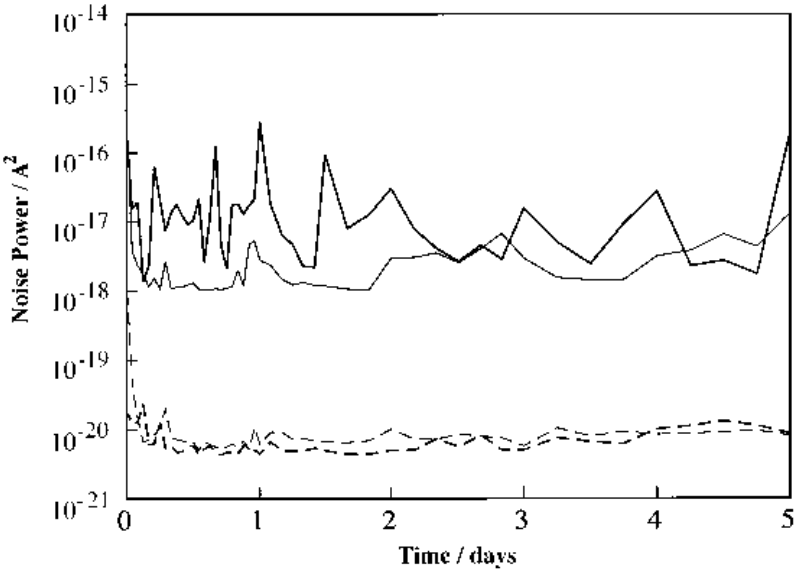

Fig. 10. Noise power values, measured at different immersion times in 0.1 M NaCl, in the absence and in the presence of tetrathiotungstate. Key: (——) AA 2014 blank; (- - - -) AA 2014 inhib.sol.; (——) AA 2014 MMC blank; (- - - -) AA 2014 MMC inhib.sol.

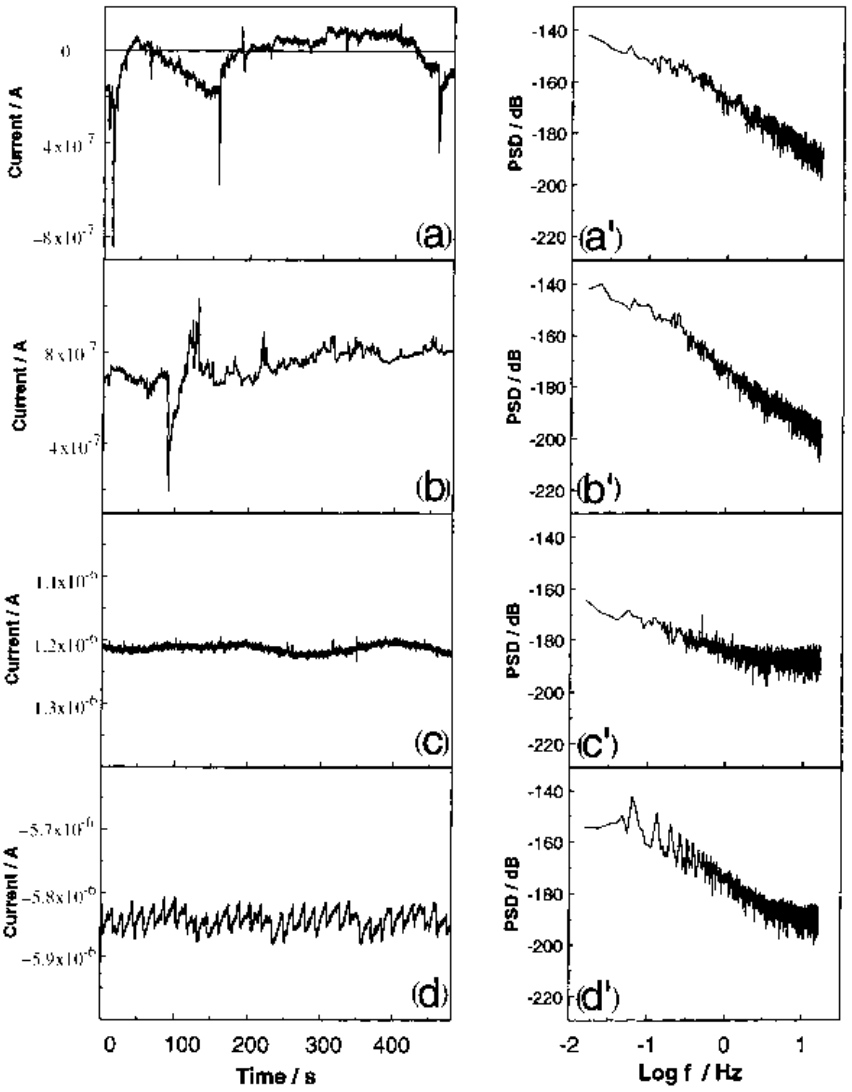

Fig. 11. Current noise data obtained after 1 day of exposure to 0.1 M NaCl solution, on AA 6061-T6 (a, a′), AA 6061-T6 MMC (b, b′), AA 2014-T6 (c, c′) and AA 2014-T6 MMC (d, d′) coupled electrodes. The data are presented both in the time domain (a, b, c, d) and in the frequency domain (a′, b′, c′, d′).

by many current transients. From the frequencies at the knees in the PSD plots, it is possible to evaluate their time constants [4–6] which fall around 0.6–0.7 s. The time records achieved with AA 2014-based materials are different from each other: the matrix produces high frequency current oscillations of small amplitude superimposed on a rather high galvanic current. In the region characterized by a $f^{-\alpha}$ trend, the corresponding spectrum has a slope of -8 dB decade^{-1}. α values smaller than 8 dB decade^{-1} were also obtained. In contrast, the composite shows many quasiperiodic peaks, with an occurrence rate of about 0.06 s^{-1} and lasting about 15 s. The corresponding spectrum shows a clear slope change at 0.075 Hz, which corresponds to the presence of current transients with repassivation time constants of about 2 s, superimposed over the saw-teeth peaks. The spectra corresponding to aperiodic time records are characterized by either linear trends ($\alpha \simeq 20$–23 dB decade^{-1}) or by very low cut off frequencies ($\tau \geq 2$ s).

At the end of the 5 day immersion (Fig. 12), more or less periodic peaks occur on both the composites and begin also to appear on AA 2014-T6. The occurrence rate depends on the matrix, as on AA 2014-based materials it is always around 0.05–0.07 s^{-1}, while it is about 0.008 s^{-1} on AA 6061-T6 MMC. The time constant of the transients occurring on AA 2014-T6 and its composite are about 3 s and 5 s, respectively. Longer time constants cannot be evaluated, within the frequency range investigated. The linear portions of the spectra of Fig. 12(c′) and (d′) exhibit α values around 18–20 dB decade^{-1}.

Knees in the spectra of Fig. 12 (a′) and (b′), obtained on AA 6061-based materials, fall at about 0.3–0.4 Hz, corresponding to current transient lifetimes of 0.4–0.5 s. Such small values cannot refer to the time constants of the repetitive current transients obtained on the composite, which are around 15 s, as evaluated from the time record. They characterize the faster transients visible in Fig. 12(b), superimposed to the repetitive ones.

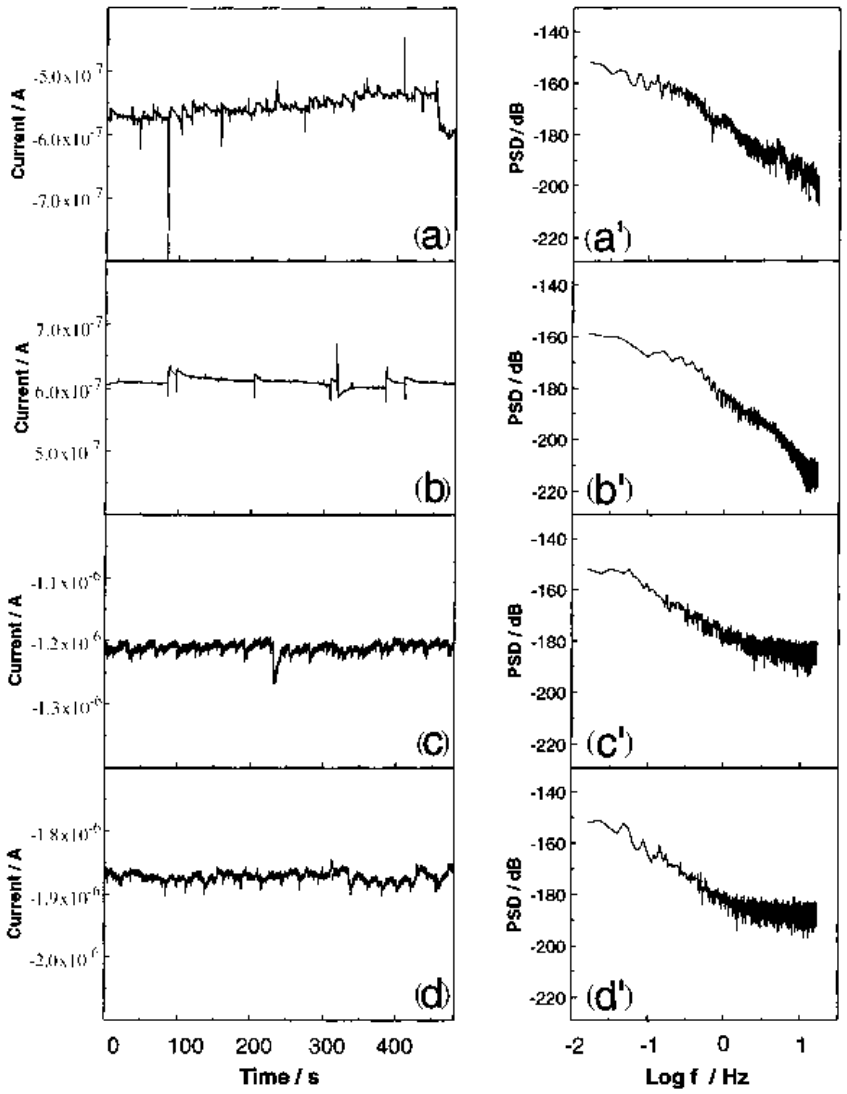

Fig. 12. Current noise data obtained after 5 days of exposure to 0.1 M NaCl solution, on AA 6061-T6 (a, a′), AA 6061-T6 MMC (b, b′), AA 2014-T6 (c, c′) and AA 2014-T6 MMC (d, d′) coupled electrodes. The data are presented both in the time domain (a, b, c, d) and in the frequency domain (a′, b′, c′, d′).

An attempt was made to evaluate possible longer time constants. The usual procedure consisted in extracting from each time record reported in the Figs 11 and 12, four time records to produce, by averaging, one spectrum with a finer structure. Therefore, the low frequency limit was decreased fourfold, by increasing the observation interval of the same amount and giving up any averaging procedure: that is, from each data file, 4096 readings were taken at a four times lower sampling frequency. In this way, it was possible to evaluate the repassivation time constants of the two matrices at 1 h of immersion: about 8 s for AA 6061-T6 and 2 s for AA 2014-T6 and to confirm the time constant values previously indicated. Time constants higher than 8–10 s cannot be evaluated.

The inhibitive effect afforded by tetrathiotungstate is clearly demonstrated by monitoring the current noise power values (Figs 9 and 10): actually, it suppresses almost any current transient in the time records, thus producing very depressed noise power values.

4. Discussion

The SEM observations and EPMA analysis could not detect the presence of intermetallic precipitates in the MMCs, indicating a more homogeneous distribution of the impurities and alloying elements in the composites than in the matrices. Therefore, in the reinforced materials, pits appear to start mainly at the alumina particle/matrix interphase, while on the matrices, a widespread micropitting attack develops around cathodic intermetallic precipitates. After 5 days of immersion, also some deep pits appear on AA 6061-T6. On the other matrix, the corrosion attack also produces intergranular pits, clearly visible at the end of 1 month of exposure to the chloride solution.

The electrochemical current noise data obtained at short immerison times in the blank solution (e.g., 1 h) indicate that pitting corrosion develops on all the materials, without a measurable induction time. This is indicated by the presence, just after the immersion, of many overlapping current transients in the time records, whose time constants, τ, depend on the re-

passivation ability of the material: at such a short immersion time, the longer τ values for AA 6061-T6 (about 8 s, than for AA 2014-T6 (about 2 s) probably depend on the efficiency of the cathodic reaction, which is much higher on the latter, as confirmed by the polarization curves (Figs 1and 2). At longer immersion times a marked decrease in the transient lifetimes on AA 6061-based materials was detected (τ values down to 0.4–0.5 s), in spite of the development of a concomitant stable pitting attack. This phenomenon was noticed on pure aluminium-based composites, reinforced with either silicon carbide particles or alumina particles [1] and was attributed to the permanence of break-heal events on the passive surface film, even during stable pit growth. The healing of passive film flaws can be made quicker as the corrosion process goes on, by emersion of cathodic impurities and/or phases. Stable pits are probably responsible of slower current oscillations, whose duration is behind the capability of the technique, with the adopted operating parameters [1]. In contrast, AA 2014-based materials exhibit rather constant repassivation times which slightly increase towards the end of the immersion period (from 2 to 5 s or more), suggesting a tendency of these materials to transform pitting attack into a general attack. The SEM micrographs taken after 5 days of immersion appear in agreement with this hypothesis as AA 2014-T6 shows a high density of micropits (Figure 5), while a widespread attack around the reinforcing particles is detected on AA 2014-T6 MMC (Fig. 6).

The analysis of the time records and their corresponding spectra can be a useful tool to evaluate the degree of localization of the corrosion attack. In fact, as suggested by other authors [7,8], the slope of the linear portion of the PSD plots is found to tend to zero (white noise) in the presence of a uniform corrosion attack. This was the case of AA 2014-T6, during the initial days of immersion. The corresponding noise power values (Fig. 10) were rather high (but lower than in the presence of extensive pitting) and constant. Only towards the end of the immersion, some exponential current transients began to appear, as a consequence of a localization of the corrosion attack. The activity of stable pits is often accompanied by the presence of quasi periodic current transients.

Quasi-periodic current transients are clearly visible on both composites, after few days of immersion and on AA 2014-T6, at the end of the immersion period, often together with quicker and smaller transients. In the literature, periodic current or potential transients are often described and are mainly connected to crevice corrosion [9–14] or to stress corrosion cracking [12]. They were attributed to mass transport or diffusion restrictions [12]. In the case investigated, here such periodicity could be connected to hydrogen gas bubbling from active pits. In fact, it is possible that when the mouth of active pits is obstructed by corrosion products the outlet of hydrogen gas bubbles is blocked, unless they reach a critical size (the case of AA 2014-T6, at long immersion periods). The effect of the reinforcing particles around the pit mouth is to produce a crevice effect that hinders gas egress, after 1 or 2 days of immersion. Such periodicity is not evident on AA 6061-T6: possibly, on this metal the necessary conditions of restricted mass transport in pits do not develop, at least within the 5 days of observation.

The recovery of such current peaks is slower on AA 6061-T6 MMC ($\tau \simeq 15$ s), than on AA 2014-based materials ($\tau = 2 - 5$ s). Also the occurrence rate is higher on the latter materials ($\simeq 0.06\ s^{-1}$) than on the former one ($\simeq 0.008\ s^{-1}$). If the egress of the gas bubble from one pit corresponds to the rising portion of each quasi-periodic current transient (increase in the anodic current from the active site), the slow descent part could be due to hydrogen gas bubble reformation. Both the faster recovery and occurrence rate of repetitive peaks on AA 2014-based materials appear in agreement with their higher cathodic activity (the cathodic current densities in the blank solution are about one order of magnitude higher on AA 2014-T6 MMC, than on AA 6061-T6 MMC, Figs 1 and 2).

On all the studied materials, tetrathiotungstate appears to inhibit both the anodic and the cathodic reaction of the corrosion process. It is not known if it acts by chemisorption or by film forming. However, some observations can be made. The E_{corr} values obtained in inhibited solutions suggest it is not an oxidizing inhibitor, as they are never ennobled, with respect to the values recorded in the blank solution. Moreover, sulfur atoms, tetrahedrically disposed around tungsten [15], must play a fundamental role, as ligands, because the addition of tungstate stimulates the corrosion process.

The inhibiting efficiency of this anion is much higher on AA 2014-based materials than on AA 6061-based materials. However, if a comparison is made between Figs 1 and 2, it is observed that in the presence of the inhibitor, the polarization curves on both composites are more or less coincident: the higher efficiency obtained on AA 2014-T6 MMC is due to its lower corrosion resistance. A hypothesis was made that the inhibitor, beside inhibiting the corrosion process on aluminium, could decrease the cathodic activity on the copper-containing strengthening phases, thus levelling the behaviour of the studied materials. To confirm this, cathodic polarization curves on copper electrodes were recorded: they actually show one order of magnitude lower cathodic current densities at the potentials at which E_{corr} values of AA2014-based materials were found.

Concerning tetrathiomolybdate, the following observations, can be made. It markedly increases the corrosion potentials of AA 6061-based materials and only slightly increases those of AA 2014-based materials. It is not able to block pitting corrosion. It slightly slows down the corrosion process of AA 2014-based materials.

These findings suggest that this anion is probably reduced by AA 6061 alloy, as confirmed by the marked stimulation of the cathodic process on this alloy. The anion reduction can produce MoS_2 and sulfide anions. The aggressivity of the sulfides (particles containing sulfur and not molybdenum were actually identified on AA 6061-T6 MMC) and the semiconducting properties of MoS_2 [15], which can induce galvanic corrosion nearby, are probably the cause for the observed stimulation of the corrosion process on AA 6061-based materials. It is possible that the reduction of the anion does not occur or occurs at a lower extent on the slightly nobler AA 2014-based materials.

This would be analogous to the different behaviour observed between tungstate and molybdate: tungstate is never reported to exhibit oxidizing capabilities towards aluminium [6,17], while molybdate, which is often quoted as a non oxidizing inhibitor for aluminium [16, 18], according to other authors is also present in a reduced form (Mo^{IV}) in the surface passive film of aluminium [19–21].

5. Conclusions

The following conclusions can be drawn:

(i) The analysis of the current noise detected during the immersion of two aluminium alloy composites and the corresponding matrices, in a neutral chloride solution, suggests that the time constants of the current transients are related to the evolution in the efficiency of the cathodic reaction on the different materials.

(ii) Stable pits produce quasi-periodic current transients, probably due to a difficult outlet of hydrogen gas bubbles from pits, partially obstructed by corrosion products and/or reinforcement particles.

(iii) It is confirmed that the slope of the PSD plots is connected to the degree of localization of the corrosion attack: α values of about 20 dB decade^{-1} were always obtained when pitting corrosion was prevalent; α values tending to zero were observed when general corrosion was dominant (on AA 2014-T6, from a few hours until 3 days of immersion).

(iv) Tetrathiotungstate is an excellent inhibitor for the studied composites and matrices and particularly for AA 2014-based materials.

(v) Current noise power values are in good agreement with the $1/R_p$ values to discriminate the corrosion resistances of aluminium alloy MMCs and corresponding matrices in neutral chloride solutions, in the absence and in the presence of tetrathiotungstate.

Acknowledgements

This work was financially supported by 60% M.U.R.S.T. Funds.

References

[1] C. Monticelli, F. Zucchi, F. Bonollo, G. Brunoro, A. Frignani and G. Trabanelli, *J. Electrochem. Soc.* **142** (1995) 405.
[2] S.V. Lomakina, T.S. Shatova and L.P. Kazansky, *Corros. Sci.* **36** (1994) 1645.
[3] Annual Book of ASTM Standards, ASTM, Vol. 03.02, Designation G1-90, (1991) p. 35
[4] U. Bertocci Proceedings of the Second International Conference on 'Localized Corrosion' (edited by H.S. Issacs, U. Bertocci, J. Kruger and Z. Szklarska-Smialowska) NACE, Houston, TX (1987) p. 127
[5] C. Gabrielli and M. Keddam, *Corrosion* **48** (1992) 794.
[6] U. Bertocci and F. Huet, *ibid.* **51** (1995) 131.
[7] C. Bataillon and C. Fiaud, Elelctrochemical Methods in Corrosion Research' (edited by M. Duprat), Materials Science Forum, vol. 8, (1986) p. 141.
[8] N. Celati and C. Bataillon, Proceedings of EUROCORR 91 (edited by I. Karl and M. Bod), Budapest (1991) p. 701.
[9] K. Hladki and J.L. Dawson, *Corros. Sci.* **21** (1981) 317.
[10] Idem, *ibid.* **22** (1982) 231.
[11] S Magaino, A. Kawaguchi, A. Hirata and T. Osaka, *J. Electrochem. Soc.* **134** (1987) 2993.
[12] D.A Eden, A.N. Rothwell and J.L. Dawson, Corrosion 91, paper 444, Cincinnati (1991).
[13] C. Monticelli, A. Frignani, G. Brunoro, G. Trabanelli, F. Zucchi and M. Tassinari, *Corros. Sci.* **35** (1993) 1483.
[14] C. Monticelli, M.C. Boggiani and F. Zucchi, Proceedings, of the 8th European Symposium on Corrosion inhibitors,' Ann. Univ., Ferrara, N.S., Sez. V, suppl. 10, (1995) p. 45.
[15] F. Jellinek, *in* Inorganic Sulphur Chemistry' (edited by G. Nickless), Elsevier Amsterdam, (1968) p. 670.
[16] R.C. McCune, R.L. Shilts and S.M. Ferguson, *Corros. Sci.* **22** (1982) 1049.
[17] C. Monticelli, G. Brunoro, F. Zucchi and F. Fagioli, *Werkst. Korros.* **40** (1989) 393.
[18] A.Kh. Bairamov, S. Zakipour and C. Leygraf, *Corros. Sci.* **25** (1985) 69.
[19] B.A. Shaw, G.D. Davis, T.L. Fritz and K.A. Olver, *J. Electrochem. Soc.* **137** (1990) 359.
[20] W.C. Moshier and G.D. Davis, *Corrosion* **46** (1990) 43.
[21] W.C. Moshier, G.D. Davis and G.O. Cote, *J. Electrochem. Soc.* **133** (1990) 1063.